

Scattering of Coherent Light by a Statistical Medium*

F. T. ARECCHI

CISE-Centro Informazioni Studi Esperienze, Milano, Italy and Università di Milano, Milano, Italy

AND

M. GIGLIO AND U. TARTARI

Università di Milano, Milano, Italy

(Received 19 May 1967)

By the joint use of a coherent light source and of photon counting statistics, we have verified the statistical properties of Brownian motion. The light source is a helium-neon laser emitting at 6328 Å. The scattering media are dilute solutions of monodisperse polystyrene spherical particles with diameters ranging from 0.088 to 1.06 μ . Three types of results are presented. First, by working at a density of scattering centers such that neither particle correlations nor multiple scattering processes have any influence, we measure the angular distributions of the field scattered by single particles, and verify the Mie theory. Second, by frequency measurements, we show the Lorentzian character of the scattered light spectrum, as one would expect from the diffusion approximation. Third, by use of photocount distributions, we measure the ensemble distribution of the scattered field within a coherence area and time, and show that the field distribution is Gaussian. The last two results imply that the field scattered by Brownian particles is accurately described as a stochastic Markov process. The techniques here used open the way to similar measurements on more complicated scattering media.

1. INTRODUCTION

RECENTLY, a great deal of information on physical systems has been obtained by scattering experiments using a laser as a source of known properties and then measuring the frequency spectra of the scattered light.¹⁻⁸ These experiments have led to extremely interesting results. However, they yield only the value of a particular parameter, namely the first-order correlation function of the density fluctuations, related by a Fourier transform to the measured power spectra of the scattered light.^{9,10}

It seems worth while to increase the information on the statistical properties of the scattering medium by using the method of photocount distributions in the study of the scattered light, either to explore the ensemble distribution within a coherence time of the material fluctuations^{11,12} or to get full information on the time

properties, complementing the frequency measurements by measurements of the joint photocount distributions.¹³ Recently extensive theoretical and experimental work has been done on the use of the statistical distributions of the photon counts from a photodetector as a tool to explore the statistical properties of an electromagnetic (EM) field.¹⁴⁻¹⁷ The photocount-distribution method has thus far mainly been applied to the study of a laser field^{11,12,18} and only in one case to a scattering problem, namely the very simple case of a rotating ground-glass scatterer.^{11,13,19}

In this work we have studied, both by photocount distributions and frequency measurements, the light scattered by a very simple statistical medium, that is,

¹² F. T. Arecchi, A. Berné, A. Sona, and P. Burlamacchi, *IEEE J. Quantum Electron.* **2**, 341 (1966); F. T. Arecchi, *Suppl. Nuovo Cimento* **4**, 756 (1966).

¹³ F. T. Arecchi, A. Berné, and A. Sona, *Phys. Rev. Letters* **17**, 260 (1966).

¹⁴ L. Mandel, *Proc. Phys. Soc. (London)* **72**, 1037 (1958).

¹⁵ R. J. Glauber, in *Quantum Optics and Electronics*, edited by C. De Witt, Blandin, and Cohen-Tannoudji (Gordon and Breach, Science Publishers, Inc., New York, 1964), pp. 109-185; in *Physics of Quantum Electronics*, edited by P. L. Kelley, B. Lax, and P. E. Tannenwald (McGraw-Hill Book Company, Inc., New York, 1966), pp. 788-811.

¹⁶ P. L. Kelley and W. H. Kleiner, *Phys. Rev.* **136**, 316 (1964).

¹⁷ Preliminary experimental work has been carried independently and simultaneously by four groups: Massachusetts Institute of Technology (MIT) [C. Freed and H. A. Haus, in *Physics of Quantum Electronics*, edited by P. L. Kelley, B. Lax, and P. E. Tannenwald (McGraw-Hill Book Company, Inc., New York, 1966), pp. 715-724; *Phys. Rev.* **141**, 287 (1966)]; Centro Informazioni Studi Esperienze (C.I.S.E.) Laboratory (see Ref. 11-13); International Business Machine Corporation (IBM) [A. W. Smith and J. A. Armstrong, *Phys. Letters* **19**, 650 (1966)]; Royal Radar Establishment (R.R.E.) (F. A. Johnson, T. P. McLean and E. R. Pike, in *Physics of Quantum Electronics*, edited by P. L. Kelley, B. Lax, and P. E. Tannenwald (McGraw-Hill Book Company, Inc., New York, 1966) pp. 706-714. Detailed information on the experimental features of the method can be found in Ref. 12.

¹⁸ C. Freed and H. A. Haus, *Phys. Rev.* **141**, 287 (1966). See also the works of MIT and IBM Groups in Ref. 17.

¹⁹ W. Martienssen and E. Spiller, *Phys. Rev.* **145**, 285 (1966).

* Work partially supported by the C.N.R. (Consiglio Nazionale delle Ricerche).

¹ H. Z. Cummins, N. Knable, and Y. Yeh, *Phys. Rev. Letters* **12**, 150 (1964).

² R. Y. Chiao and B. P. Stoicheff, *J. Opt. Soc. Am.* **54**, 1286 (1964).

³ J. B. Lastovka and G. B. Benedek, *Physics of Quantum Electronics*, edited by P. L. Kelley, B. Lax, and P. E. Tannenwald (McGraw-Hill Book Company, Inc., New York, 1966), p. 231-240.

⁴ S. S. Alpert, D. Balzarini, A. Novik, L. Seigel, and Y. Yeh, *Physics of Quantum Electronics*, edited by P. L. Kelley, B. Lax, and P. E. Tannenwald (McGraw-Hill Book Company, Inc., New York, 1966), pp. 253-259.

⁵ N. C. Ford, Jr., and G. B. Benedek, *Phys. Rev. Letters* **15**, 649 (1965).

⁶ T. J. Greytak and C. B. Benedek, *Phys. Rev. Letters* **17**, 179 (1966).

⁷ G. B. Benedek and K. Fritsch, *Phys. Rev.* **149**, 647 (1966).

⁸ J. B. Lastovka and G. B. Benedek, *Phys. Rev. Letters* **17**, 1039 (1966).

⁹ L. I. Komarov and I. Z. Fisher, *Zh. Eksperim. i Teor. Fiz.* **43**, 1927 (1962) [English transl.: *Soviet Phys.—JETP* **16**, 1358 (1963)].

¹⁰ R. Pecora, *J. Chem. Phys.* **40**, 1604 (1964).

¹¹ F. T. Arecchi, *Phys. Rev. Letters* **15**, 912 (1965); F. T. Arecchi, A. Berné, and P. Burlamacchi, *ibid.* **16**, 32 (1966).

a collection of equal-size spherical Brownian particles. We have chosen to make the first experiment a simple one, for which a complete theoretical treatment is already available.^{10,20,21} In Sec. 2, we briefly recall the main points of the scattering theory at optical frequencies, partly adapting the theory developed for thermal-neutron scattering,²⁰⁻²² and partly using some recent treatments for the optical field.^{7,9,10} In Sec. 3 we describe the experimental arrangement, and illustrate the peculiar problems which distinguish a photocount distribution measurement from a simpler frequency measurement. In our case (system of equal uncorrelated particles), the absence of a "two-particle" correlation part in the density correlation function (see Sec. 2) allows us, as a byproduct, to give detailed angular-distribution measurements for the single scatterer. These are shown in Sec. 4, and they fit the values computed by the Mie theory.²³ Sections 5 and 6 give the results of photocount and frequency measurements. These measurements are in agreement with the theoretical predictions for the scattered field, that is, we obtain a Gaussian ensemble distribution for the field observed within a coherence time and area, and a Lorentzian line profile for the field-power spectrum. This last result shows that the diffusion approximation is sufficient when studying scattering from Brownian particles at optical frequencies.

2. THEORETICAL CONSIDERATIONS

Before the introduction of laser sources, the scattering of light by identical particles was studied in the "static approximation." This corresponds to considering the energy transfer in the scattering process as small compared to the energy of the scattered photon. In this case the intensity of the scattered field in the direction of vector \mathbf{k}_s is given by

$$I(\mathbf{K}) = A(\mathbf{K}) \int_V e^{-\mathbf{K} \cdot \mathbf{r}} G(\mathbf{r}) d\mathbf{r}, \quad (1)$$

where $\mathbf{K} = \mathbf{k}_0 - \mathbf{k}_s$ is the difference in wave vector between incident and scattered waves, $A(\mathbf{K})$ is the scattered intensity associated with a single scatterer, and the integral is evaluated over the illuminated region. Since usually the minimum size of the illuminated region is much larger than $1/K$, we can extend the integration limits up to infinity, and the integral becomes the Fourier transform of the radial density distribution function $G(\mathbf{r})$. This function describes the mean density of particles around a given particle, and can be thought of as the probability that, if the par-

ticule is at the origin, another particle will be at point \mathbf{r} at the same time. We note that in relation (1) there is a very clear distinction between the contribution of the single scatterer and the interference contribution of the different scatterers.

Recently, the introduction of the very monochromatic laser sources and the development of optical and electronic high-resolution spectroscopy, has allowed an extension of the time-dependent theory to light scattering. The time-dependent theory of scattering has been developed by Glauber^{20,22} and Van Hove²¹ in the case of thermal-neutron scattering, and later adapted by Komarov and Fisher⁹ and by Pecora¹⁰ to photon scattering.

In these theories, taking into account only single scattering events, Eq. (1) is generalized by a relation between the spectral density $I(\mathbf{K}, \Delta\omega)$ of the scattered field $\mathbf{E}(\mathbf{K}, t)$, defined as the Fourier transform of the field correlation function

$$I(\mathbf{K}, \Delta\omega) = \int_{-\infty}^{\infty} dt e^{-i\Delta\omega t} \langle \mathbf{E}^*(\mathbf{K}, 0) \cdot \mathbf{E}(\mathbf{K}, t) \rangle \quad (2)$$

(where the angular brackets denote an ensemble average, and $\Delta\omega$ is the frequency difference between incident and scattered fields), and the density correlation function $G(\mathbf{r}, t)$, defined as

$$G(\mathbf{r}, t) = \frac{1}{N} \int_V \sum_{i,j=1}^N \langle \delta(\mathbf{r}' - \mathbf{r}_i(0)) \delta(\mathbf{r}' + \mathbf{r} - \mathbf{r}_j(t)) \rangle d\mathbf{r}', \quad (3)$$

where N is the total number of scattering particles, and the brackets denote an average over the equilibrium joint distribution of the random variables $\mathbf{r}_i(0)$ and $\mathbf{r}_j(t)$ (particle positions at different times). The generalized relation is

$$I(\mathbf{K}, \Delta\omega) = A(\mathbf{K}) \int d\mathbf{r} e^{-i\mathbf{K} \cdot \mathbf{r}} \int dt e^{-i\Delta\omega t} [G(\mathbf{r}, t) - \rho_0], \quad (4)$$

where $A(\mathbf{K})$ is the same as in Eq. (1) and ρ_0 is the average density of the medium.

It is now convenient to split $G(\mathbf{r}, t)$ into a "single-particle" function $G_s(\mathbf{r}, t)$ and a "two-particle" function $G_d(\mathbf{r}, t)$, corresponding, respectively, to the terms $i=j$ and $i \neq j$ in the sum (3). The former gives the probability that the same particle that was at $(0,0)$ will be found at (\mathbf{r}, t) , while the latter gives the probability of finding at (\mathbf{r}, t) a particle different from the one which was at $(0,0)$. $G_s(\mathbf{r}, t)$ clearly describes the wandering of a given particle away from its initial position.

In the static approximation the single-particle and two-particle correlation functions reduce, respectively, to

$$\begin{aligned} \lim_{t \rightarrow 0} G_s(\mathbf{r}, t) &= \delta(\mathbf{r}), \\ \lim_{t \rightarrow 0} G_d(\mathbf{r}, t) &= (1/N) \sum_{i,j} \langle \delta(\mathbf{r} + \mathbf{r}_i - \mathbf{r}_j) \rangle = G(\mathbf{r}). \end{aligned} \quad (5)$$

We now apply these considerations to the case of scattering from Brownian particles. In this case the corre-

²⁰ R. J. Glauber, Phys. Rev. **87**, 189 (1952); **94**, 751 (1954).

²¹ L. Van Hove, Phys. Rev. **95**, 249 (1954).

²² R. J. Glauber, in *Lectures in Theoretical Physics*, edited by W. E. Brittin *et al.* (Interscience Publishers, Inc., New York, 1962), Vol. IV, pp. 571-615.

²³ G. Mie, Ann. Physik **25**, 377 (1908); H. H. Denman, W. J. Pangonis, and W. Heller, *Angular Scattering Functions for Spheres* (Wayne State University Press, Detroit, Michigan, (1966).

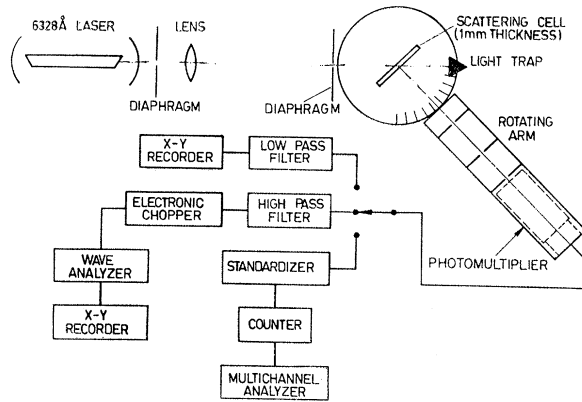


FIG. 1. Schematic representation of the experimental setup. The three different electronic chains correspond to different measurements, namely (from top to bottom). (a) angular intensity distributions, (b) frequency spectra, and (c) photocount distributions.

lation function $G(\mathbf{r}, t)$ can be determined by the following arguments. If we neglect the density fluctuations in the dispersing liquid, then scattering will arise from the fluctuations in space and time of the excess dielectric constant of the solution, i.e., the dielectric constant of the particles minus that of the pure liquid. These fluctuations are induced by the random motion of particles inside the medium. In the classical theory of Brownian motion, the particles are always supposed to be uncorrelated, that is, the motion of one particle has no influence on the remaining ones. Hence $G(\mathbf{r}, t)$ reduces to a single-particle function $G_s(\mathbf{r}, t)$.

For the Brownian motion, the time-averaged scattered intensity measured at a given direction is related in a straightforward way to the intensity scattered by a single particle. In fact the time average of the intensity is given by the field correlation function $\langle \mathbf{E}^*(\mathbf{K}, 0) \cdot \mathbf{E}(\mathbf{K}, t) \rangle$ specialized to $t=0$. A comparison of relations (2) and (4) shows that this is the space Fourier transform of the density correlation function taken in the static approximation. But in our case this is a δ function, whose angular spectrum is uniform. Therefore, the angular distribution is given by $A(\mathbf{K})$, that is, the measured pattern yields information on the geometry of the single scatterer. Since we make experiments on homogeneous dielectric spheres, we may use the classical results given by Mie.²³

Let us now look at the time behavior. A relation for the frequency distribution of the light scattered at a given angle can be obtained by performing the space-time Fourier transform of $G_s(\mathbf{r}, t)$. Therefore we need an explicit expression for $G_s(\mathbf{r}, t)$. In the theory of the Brownian motion the velocity \mathbf{u} of the center-of-mass of the particle obeys a Langevin equation

$$\frac{d\mathbf{u}}{dt} + \beta\mathbf{u} = \mathbf{F}(t). \quad (6)$$

Here $\mathbf{F}(t)$, the noise force per unit mass, is a Gaussian

stochastic process correlated on a very short time scale, that is,

$$\langle \mathbf{F}(0) \cdot \mathbf{F}(t) \rangle = C\delta(t), \quad (7)$$

(C being a constant), and β is the friction constant divided by the mass m of the particle, given by the Stokes formula

$$\beta = 6\pi a\eta/m, \quad (8)$$

where a is the radius of the particle and η the viscosity coefficient of the water.

The solution of this stochastic problem provides the conditioned probability $P_c(\mathbf{r}, t; \mathbf{r}_0, t_0; \mathbf{u}_0 | \mathbf{r}t)$ that a particle will be at (\mathbf{r}, t) if it was at (\mathbf{r}_0, t_0) with a velocity \mathbf{u}_0 . A full treatment can be found in Ref. 24. Remembering its definition, $G_s(\mathbf{r}, t)$ can be deduced from $P_c(\mathbf{r}, t; \mathbf{r}_0, t_0; \mathbf{u}_0 | \mathbf{r}t)$. By performing an integration over the initial velocities one obtains the following relation:

$$G_s(\mathbf{r}, t) = \frac{1}{[\pi\sigma^2(t)]^{3/2}} e^{-r^2/\sigma^2(t)}. \quad (9)$$

This is a Gaussian in r , with a time-dependent mean-square deviation given by

$$\sigma^2(t) = \frac{4k_B T}{m\beta^2} (e^{-\beta|t|} + \beta|t| - 1), \quad (10)$$

where k_B is Boltzmann's constant and T the temperature of the surrounding liquid. For large values of $|t|$, the function $\sigma^2(t)$ becomes

$$\sigma^2(t) = 4(D|t| - mD^2/k_B T), \quad (11)$$

where D is a diffusion constant, related to the friction coefficient by the Einstein relation

$$D = k_B T / m\beta. \quad (12)$$

The space-Fourier transform of relation (9) is given by

$$G_s(\mathbf{k}, t) \exp = \{ -(K^2 D / \beta) (e^{-\beta|t|} + \beta|t| - 1) \}.$$

This exponential can be expanded in a series with respect to the parameter $\gamma = K^2 D / \beta$. The scattered spec-

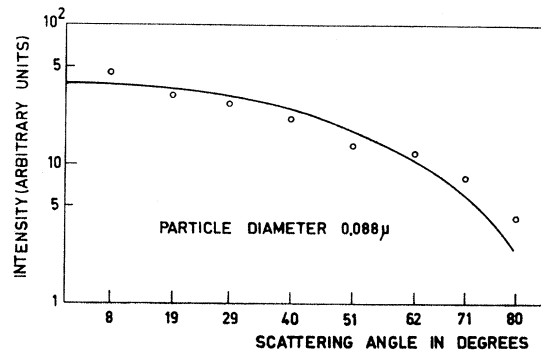


FIG. 2. Angular scattering diagram for particles of 0.088- μ diameter.

²⁴ S. Chandrasekhar, Rev. Mod. Phys. 15, 1 (1943).

tral density is obtained using Eq. (4), by a time-Fourier transformation of each term of the series. The result is

$$I(\mathbf{K}, \Delta\omega) = A(\mathbf{K}) \sum_{l=0}^{\infty} \frac{1}{l!} \left(-\frac{K^2 D}{\beta} \right)^l \frac{K^2 D + l\beta}{\Delta\omega^2 + (K^2 D + l\beta)^2}. \quad (13)$$

In the usual operating conditions, $\gamma \ll 1$. Therefore, only the $s=0$ term is important in determining the experimental results, and $I(\mathbf{K}, \Delta\omega)$ can be approximated by a single Lorentzian

$$I(\mathbf{K}, \Delta\omega) = A(\mathbf{K}) \frac{K^2 D}{\Delta\omega^2 + (K^2 D)^2}. \quad (14)$$

Typical values, for a particle of polystyrene of radius $a=0.25\mu$ and for a scattering angle of 40° , are

$$\begin{aligned} K &= 0.9 \times 10^5 \text{ cm}^{-1}, \\ D &= 0.9 \times 10^{-8} \text{ cm}^2 \text{ sec}^{-1}, \\ \beta &= 7 \times 10^{10} \text{ sec}^{-1}. \end{aligned}$$

This leads to a value $\gamma \approx 10^{-9}$ for the expansion parameter in Eq. (13).

So far, we have discussed mainly Eq. (4), which is a relation between the scattered intensity and a particular average referring to the medium, that is, the first-order correlation function of the particle's position. More information could be obtained if the ensemble distribution of the scattered field were known. This point will be discussed in Sec. VI.

3. EXPERIMENTAL ARRANGEMENT

Three different kinds of measurements on the light scattered by a solution of dielectric particles in Brownian motion have been performed: (a) angular intensity distributions, (b) frequency distributions at fixed scattering angles, and (c) photocount distributions.

The experimental arrangement, shown in Fig. 1, consists of the light source, the scattering cell with the collecting optics, and the electronics for the three types of experimental analyses to be performed. The light source is a 6328-Å He-Ne gas laser delivering 2 mW when operating in the TEM₀₀ mode. The output power is monitored to avoid long-term drifts. The beam di-

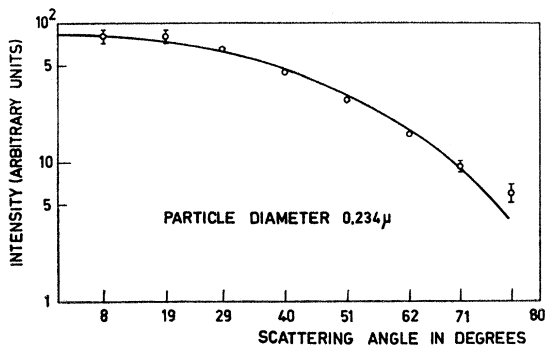


Fig. 3. Angular scattering diagram for 0.234- μ diameter.

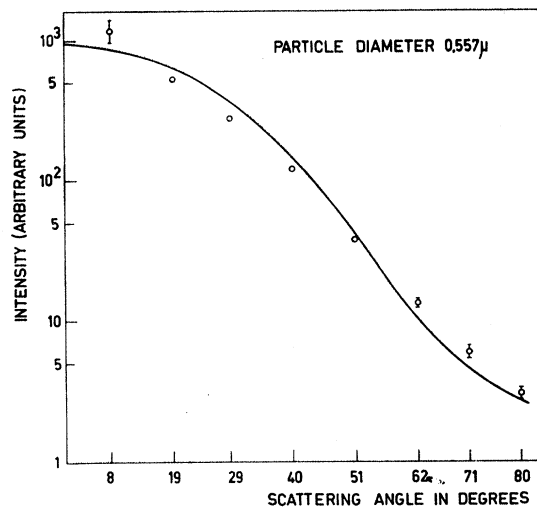


Fig. 4. Angular scattering diagram for 0.557- μ diameter.

ameter is reduced to about 0.2 mm by the use of a lens with a long focal length. A very thin (1 mm) scattering cell is introduced into the laser beam at the Brewster angle. The small over-all transverse dimensions of the interacting volume provide fairly large coherence areas for the scattered light, which are nearly constant even for large off-axis scattering angles. In such a way, a pinhole diaphragm of practical aperture size can be used to collect the scattered light within a coherence area. Stray light has been carefully eliminated by means of diaphragms. The laser beam after passing through the cell is extinguished by a light trap.

The measurements are performed on dilute solutions of monodisperse polystyrene spherical particles²⁵ with different diameters from 0.088 to 1.06 μ . Each sample is composed of almost equal-size particles, with a very small variance. The liquid in which the particles are dispersed is deionized water, filtered with a Millipore filter. The attenuation of the beam through the cell never exceeds 15%, so that the multiple scattering contributions can be neglected. Furthermore, knowing the scattering cross section and the cell depth, we can evaluate the average mutual distance between the polystyrene spheres. This turns out to be always much larger than a wavelength, so that no fixed phase correlation exists between the elementary wavelets scattered by the spheres, and the scattering contributions can be considered as independent. A further point should be emphasized regarding the small scattering volume. Discrepancies between experimental results and the plane-wave approach to the scattering should be expected when the escape time of the particles from the interaction volume is smaller than the characteristic relaxation time for the momentum of the particles, defined as the average time interval which elapses before collisions make a particle forget its initial velocity. This

²⁵ The polystyrene latex samples have been kindly provided by the Dow Chemical Company.

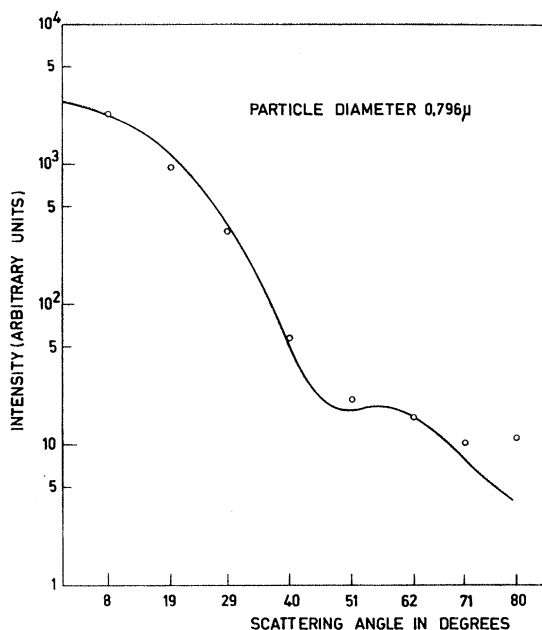


Fig. 5. Angular scattering diagram for 0.796- μ diameter.

time is equal to β^{-1} , where β is defined in Eq. (8). In our case the escape time can be evaluated on the basis of the diffusion theory for the Brownian particle, and typical values are larger than 10^{-1} sec, whilst the relaxation time β^{-1} is of the order of 10^{-10} sec. Hence the plane-wave theory applies in spite of the small diameter of the incident beam. To evaluate the real scattering angle inside the cell, corrections for refractions must be taken into account. Minor corrections are needed for the variations in the solid angle of collection and the reflectivity of the cell boundaries at different scattering angles. These corrections become important only for large emergence angles. We have confined ourselves to the study of forward scattering, since for large particle diameters, the back reflection of the forward lobe masks the backscattered lobe. If particular care is not taken, stray light from the edges of the cell and light due to internal reflections could constitute the major contributions to the collected light, particularly at large off-axis angles. These spurious contributions are eliminated by an efficient light trap selecting a very narrow solid angle of collection centered on the interaction volume.

We have used different photodetectors for photocount distributions and for frequency and angular distributions. In the first case, it is important to have a single photoelectron pulse high enough to exceed the threshold of a nonlinear circuit (see Sec. 6); therefore we have used a 56 AVP photomultiplier with an S-11 photocathode (0.5% quantum efficiency at 6328 Å) and 14 dynodes, operated at high voltage, so that the average gain is 10^3 . In the second case, it is important to reduce the shot noise; hence we have used an XP 1002 photo-

multiplier, with an S-20 photocathode (5% quantum efficiency) and only 10 dynodes. In all cases, no filters were employed, and the photocathode was at 50 cm from the scattering cell with a circular diaphragm of 0.5-mm diameter in front of it.

4. ANGULAR DISTRIBUTIONS

Performing a time average on the scattered intensity, we obtain the angular intensity distribution for the scattered light, as discussed in Sec. 2. Since there are no correlations between particles, the angular distribution is expressed in terms of the single-particle scattering theory, as given by Mie.²³ For a given angle φ , related to K by the relation $K = (4\pi/\lambda)\sin^2(\frac{1}{2}\varphi)$, the intensity of the scattered light depends on two parameters, q and m . The first, $q = \pi d/\lambda$, is the ratio between the particle diameter d and the wavelength of the light in the surrounding medium (water); the second is the relative refraction index, which is 1.199 for polystyrene in water.

The fluctuating output photocurrent was fed to an X-Y recorder through a low-pass filter. The results are shown in Fig. 2-6. The experimental points agree with the nearest values of q and m among the published values.²³ The dispersion of the experimental data is less than 5% for all measurements. A few points in large disagreement with the theoretical curves are thought to be due to some residual systematic error (anomalous refractions from cell irregularities for particular positionings of the cell). The size of the error line associated with each experimental point corresponds to the maximum dispersion over three runs.

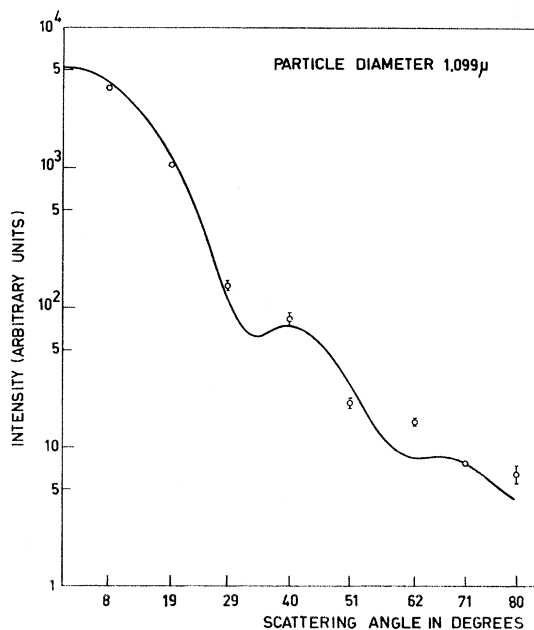
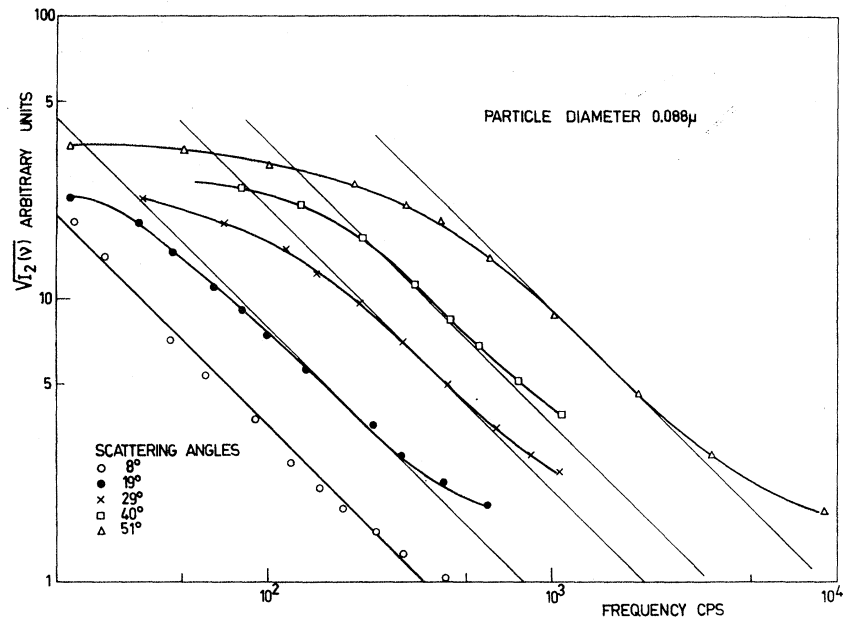


Fig. 6. Angular scattering diagram for 1.099- μ diameter.

FIG. 7. Square root of the photo-current power spectrum: particle diameter 0.088 μ .



5. FREQUENCY SPECTRA

The series expansion (13) provides a full expression for the power spectrum of the light scattered at a given angle. All terms besides the first may be safely omitted in our case, since the parameter $\gamma = K^2 D / \beta$ in the power expansion is of the order of 10^{-9} . In this diffusion approximation the Lorentzian line emerges. Since linewidths of a few cps are expected, very-high-resolution techniques are required.

We have used the self-beat technique.⁵ This technique permits a knowledge of the spectrum $I_1(\omega)$ of the scattered light from the knowledge of the spectral distribution $I_2(\omega)$ of the fluctuations in the output of a photodetector collecting light within a coherence area.²⁶ $I_1(\omega)$ and $I_2(\omega)$ are the Fourier transforms of the correlation function of the field and of the intensity fluctuations, respectively, i.e.,

$$I_1(\omega) = \int dt e^{-i\omega t} \langle E^*(0) \cdot E(t) \rangle, \quad (15)$$

$$I_2(\omega) = \int dt e^{-i\omega t} \langle |\delta E(0)|^2 |\delta E(t)|^2 \rangle,$$

where $\delta E = E - \langle E \rangle$. For Gaussian processes, the second correlation function is equal to the square of the first,²⁷ hence the two frequency spectra are related by a con-

²⁶ This is not necessary in these measurements. In fact, working in a region larger than a coherence area means only adding a further dc contribution, i.e., increasing the δ function centered at zero frequency. However, the limitation becomes necessary when measuring photocount statistics.

²⁷ M. C. Wang and C. E. Uhlenbeck, Rev. Mod. Phys. 17, 329 (1954).

volution formula²⁸

$$I_2(\omega) = \int_{-\infty}^{\infty} I_1(\omega') I_1(\omega - \omega') d\omega'. \quad (16)$$

Equation (16) means in practice that the spectral density at ω is the sum of all the beats between spectral components at optical frequencies differing by an amount ω . One may easily verify that if $I_1(\omega)$ is a Lorentzian centered at the frequency ω_0 , with a linewidth $\Delta\omega$, then $I_2(\omega)$ is also a Lorentzian, but centered at zero frequency and with a linewidth $2\Delta\omega$. The output voltage from a wave analyzer with a full-wave bridge, as used in our measurements, is proportional to the square root of $I_2(\omega)$, hence a square root of a Lorentzian is expected as a direct result of the measurement. Beside being simpler, the self-beat technique is more suitable than the heterodyne technique when measuring lines of a few cps in width, since the factor 2 between the linewidths of $I_2(\omega)$ and $I_1(\omega)$ can be extremely useful when working at the limit of the wave-analyzer resolution.

The linewidth (half-width at half-height) of the scattered light, as given by formula (14), is $\Delta\omega = K^2 D$ and from this one obtains the following numerical formula for its dependence on the scattering angle

$$\Delta\nu = [49 \sin^2(\frac{1}{2}\phi) / d], \quad (17)$$

where we have used the Bragg condition $K = 2k_0 \sin \frac{1}{2}\phi$ ($k_0 = 2\pi n / \lambda_0$) and the relation $D = k_B T / 3\pi d \eta$ (d being

²⁸ The self-beat technique provides a complete description only for the case of a Gaussian field. For a scattered field, the Gaussian nature can be taken for granted, as an obvious consequence of the central limit theorem, whenever one deals with linear scattering processes from uncorrelated scatterers. Direct experimental evidence of the Gaussian character of the scattered field is discussed in the following section.

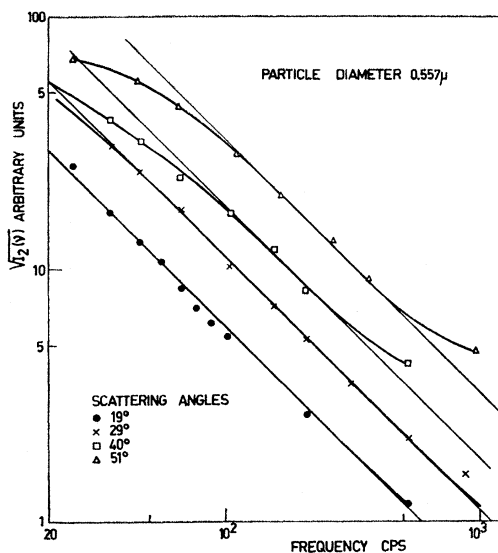


FIG. 8. Square root of the photocurrent power spectrum: particle diameter 0.557μ .

the particle diameter) resulting from Eqs. (12) and (8). The numerical coefficient results from using the values $n=1.33$ (water) $\lambda_0=6328 \text{ \AA}$, $T=293^\circ\text{K}$ (room temperature), $\eta=10^{-2}$ poise, and expressing d in microns.

The photomultiplier is the same as in the angular measurements, and the wave analyzer is a Hewlett Packard 302 A, with a bandwidth of 6 cps. The output of the wave analyzer is recorded after passage through a low pass filter (time constant 15 sec). In Fig. 7 and 8 the measured frequency spectra are given in a log-log plot, for various scattering angles. Reported measurements refer to particles with 0.088 and $0.557\text{-}\mu$ diameters. The $0.088\text{-}\mu$ -diam particles give the largest broadening, while the $0.557\text{-}\mu$ -diam particles give the smallest broadening still detectable. The shot noise makes the fitting less accurate for experimental points corresponding to large-angle scattering. Experimental data in the higher frequency region fit fairly well with a straight line of slope -1 , thus verifying the Lorentzian character of the scattered-light spectrum. However some uncertainty still remains in regard to the proper value of linewidth to be attributed to each curve, since no data can be collected in the $0\text{-}20\text{-cps}$ range because of instrumental limitations. To clarify this point, a slightly different technique has been used. The photomultiplier output has been filtered through a high-pass filter in order to remove the dc component, and electronically chopped at 1 kc/sec. In this way the power spectrum has been translated to around 1 kc/sec and the whole spectral profile can be measured. The data obtained again fit fairly well with a Lorentzian shape, and the linewidth can now be evaluated (an example is given in Fig. 9).

By this compound technique both the Lorentzian character and the agreement between measured and

expected linewidth can be checked.²⁹ The agreement seems to be fairly good for $0.088\text{-}\mu$ particles, and less accurate for $0.557\text{-}\mu$ particles, especially at low scattering angles, where a systematic deviation from the expected linewidth may be noted (see Fig. 10). This cannot be attributed to the measuring procedure, since several independent checks have always led to self-consistent results. Some, as yet, obscure systematic effect must be invoked, as for instance the local heating due to inelastic scattering of the incident light,³⁰ or a further broadening due to deviations of the single scatterers from a spherical shape.

6. PHOTOCOUNT DISTRIBUTIONS

The connection between the ensemble distribution $P(E_0)$ of the complex amplitude E_0 of a classical electromagnetic field and the photoelectron distribution $p(n)$ from a photodetector interacting with the field is given by¹⁴

$$p(n) = \frac{1}{n!} \int (\zeta |E_0|^2 T)^n e^{-\zeta |E_0|^2 T} P(E_0) d^2 E_0 \quad (18)$$

($d^2 E_0 = d(\text{Re} E_0) d(\text{Im} E_0)$) under the following assumptions:

- (1) The measuring time T is much shorter than the coherence time τ_c of the field.
- (2) The illumination is uniform over the used region of the photocathode surface.
- (3) ζ takes into account the quantum efficiency of the photocathode, eventual attenuator factors due to

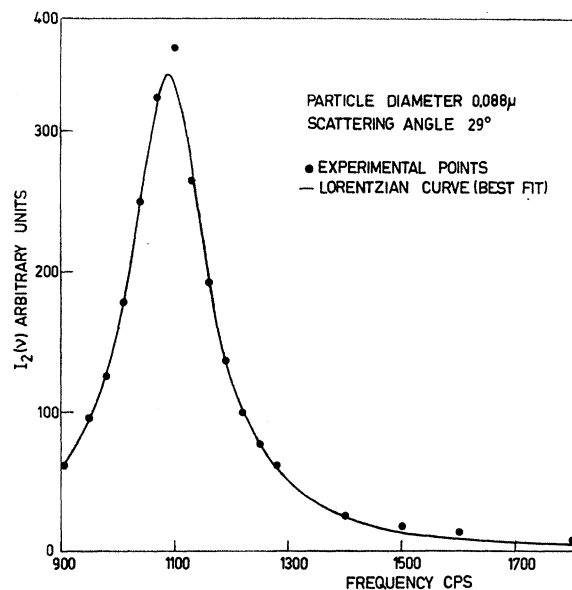


FIG. 9. Sample of a power spectrum of the chopped photocurrent.

²⁹ In a previous work (see Ref. 1), linewidths obtained by the heterodyne technique were reported, but no direct evidence was given for the Lorentzian character of the scattered light.

³⁰ K. E. Rieckhoff, Appl. Phys. Letters 9, 87 (1966).

filters, and a dimensional factor to translate from field intensity to "photon" numbers.

The relation (18) has been given a quantum-mechanical treatment by Glauber¹⁵ and by Kelley and Kleiner.¹⁶ We summarize here the main results. Let us write the field operator in a given cavity of volume V in an orthonormal-mode expansion (we consider for simplicity a single polarization and use mks units);

$$E(\mathbf{r}, t) = i \sum_k (\hbar\omega_k/2\epsilon_0 V)^{1/2} \times [a_k(t)\mu_k(\mathbf{r}) - a_k^\dagger(t)\mu_k^*(\mathbf{r})], \quad (19)$$

where $\mu_k(\mathbf{r})/\sqrt{V}$ are a complete orthonormal set of cavity eigenfunctions. Then we use the "coherent state" representation, i.e., we take the expectation value over the complete space of the eigenstates of the annihilation operators defined by¹⁵

$$a_k |\alpha_1, \alpha_2, \dots, \alpha_k, \dots\rangle \equiv a_k |\{\alpha_k\}\rangle = \alpha_k |\{\alpha_k\}\rangle. \quad (20)$$

In this way we obtain a relation similar to Eq. (18), where now the weight function is Glauber's $P(\{\alpha_k\})$, which appears as a weight function in the diagonal representation of the field density operator

$$\rho = \int |\{\alpha_k\}\rangle \langle \{\alpha_k\}| P(\{\alpha_k\}) \{d\alpha_k^2\}, \quad (21)$$

where $\{d^2\alpha_k\}$ stands for $\prod_k d(\text{Re}\alpha_k)d(\text{Im}\alpha_k)$. In general we should write a relation between photocount and field distributions such as Eq. (17.35) of Ref. 15 to take into account the multimode structure of the field. However, limiting ourselves for simplicity to a single mode, and introducing a new coefficient s for quantum efficiency and attenuation, we obtain

$$p(n) = \frac{1}{n!} \int (s|\alpha|^2 T)^n e^{-s|\alpha|^2 T} P(\alpha) d^2\alpha, \quad (22)$$

which appears formally identical to the classical relation (18).

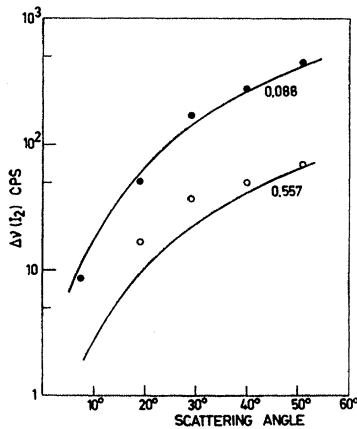


FIG. 10. Theoretical and experimental values of linewidths of the photocurrent power spectrum (full width at half-height).

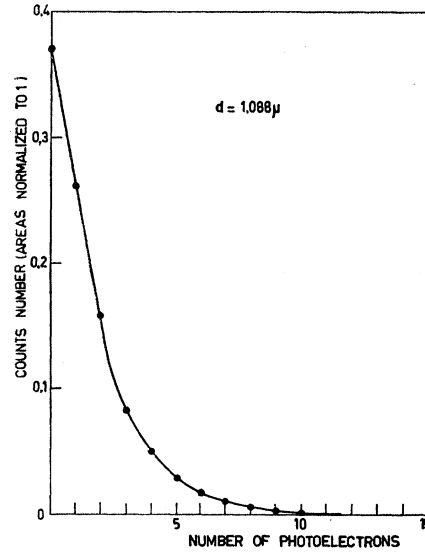


FIG. 11. Example of a photocount distribution as obtained performing measurements within a coherence area and a coherence time.

This relation permits us to know the statistical distribution $P(\alpha)$ of a field once the photocount distribution $p(n)$ has been measured. A similar relation can be found between the joint field distribution for two different times and a joint photocount distribution.¹³ This way of investigating is more general than the use of relations between ensemble averages, such as Eq. (4), which relates the first-order correlation functions of the scattered field and of the scattering medium.

When we apply these considerations to the field scattered by Brownian particles, since the statistical properties of the incident laser field are already known, the measured distributions of the scattered field yield information on the properties of the medium.

The conditions under which we perform measurements on a single mode must be specified. From a spatial point of view, each scattered mode is isolated on the detector when the aperture of the detector is smaller than a coherence area A_c defined by

$$A_c \lesssim (dR/\lambda)^2, \quad (23)$$

d being the maximum size of the scattering region on a direction orthogonal to the scattered direction \mathbf{k}_s , and R the distance between the scatterer and the photodetector (this relation holds when R is much larger than the size of the scatterer). From a temporal point of view, field amplitudes for the scattered mode are correlated within a coherence time τ_c depending on the correlation time of the density fluctuations in the scattering medium. We already know from the experiments of Sec. 5 the value of this relaxation time τ_c . Therefore, it is easy to choose times much shorter than τ_c , so that the field measurements correspond to an "instantaneous" sampling over an ensemble distribution.

TABLE I. Data obtained by photocount measurements (see Fig. 11).

Particle diameter (μ)	1.088			0.796	
	Total count number	55.226	121.475	87.921	60.050
Mean value	0.763	1.489	1.754	1.294	1.820
Variance	1.328	3.580	4.695	2.881	4.976
H_2	0.97	0.95	0.94	0.94	0.955

Within these experimental limitations, the photocount distributions are given by the relation (22).

It is readily apparent, by the central limit theorem (the reasoning is very classical and was first made by Lord Rayleigh; see Ref. 11), that scattering of a coherent field from uncorrelated scatterers gives rise to a Gaussian field distribution for each scattered mode, i.e., denoting by $\langle n_k \rangle$ the photon number in the K th mode, the Glauber P function for that mode is given by

$$P(\alpha_k) = \frac{1}{\pi \langle n_k \rangle} \exp - \frac{|\alpha_k|^2}{\langle n_k \rangle}. \quad (24)$$

The associated photocount distribution, taken in the above mentioned experimental conditions, is given by a Bose-Einstein, or geometric, distribution

$$p(n) = \frac{1}{1 + \langle n_T \rangle} \left(\frac{\langle n_T \rangle}{1 + \langle n_T \rangle} \right)^n, \quad (25)$$

where $\langle n_T \rangle$ is the average number of photoelectrons detected in the time T .

We could in the same way write a relation for the joint photocount distribution, as we have done in Ref. 13. However, as discussed there, for this case of linear scattering the same information is already furnished by the frequency measurements. We therefore limit our experiments to first-order distribution functions.

The experimental arrangement for photocount measurements has already been described in Ref. 12, to which we refer the reader for details. Here we add only that the thermal noise contribution from the photocathode is reduced to a negligible value by an electronic diaphragm, which consists in giving a negative potential to the focusing electrode between the cathode and the first dynode of the 56 AVP phototube, thus reducing the effective photocathode surface to only 1 mm². Use has been made of the nonlinear method^{11,12}, i.e., we have standardized the output pulses from the photomultiplier, thus avoiding statistical spreading due to fluctuations in the multiplication process. This has been possible because the coherence times τ_c are so long that we can safely use measuring intervals T much larger than the dead time of the nonlinear circuit which performs the standardization (about 10 nsec). Experimental results are reported in Table I for spheres of diameter 1.088 and 0.79 μ . An example is shown graphically in Fig. 11.

For each run we have calculated the reduced second factorial moment

$$H_2 = [\langle n(n-1) \rangle / \langle n \rangle^2] - 1, \quad (26)$$

which goes from 1 for a Bose distribution to 0 for a Poisson distribution. We note from Table I that our measurements agree with the theoretical expectations within a few percent. The residual error cannot be attributed either to the aperture of the observation system (since this was much smaller than a coherence area) or to the measuring time. Furthermore the photocount technique has already been tested^{11,12} and is known to give no errors besides the expected uncertainty due to the finite count number, and this uncertainty is negligible in the case of the actual numbers used in our experiments. We suppose that a small non-Gaussian contribution could arise from multiple scattering. In fact, while the "primary interaction" volume is small and its size is limited by the beam diameter, the "secondary interaction" volume over which multiple scattering is effective extends to the whole cell and must be associated with coherence areas much smaller than the phototube aperture, thus introducing an uncorrelated contribution.

7. CONCLUSIONS

The results may be divided into three parts. By working at a density of scattering centers such that neither van der Waals correlations nor multiple scattering processes have any influence, we have exploited the absence of a "two-particle" density correlation function to measure the angular distributions corresponding to the light scattered by a single particle.

Then, by the joint use of photocount distributions and frequency measurements, we have shown the validity of the Markov approximation for the scattered EM field, that is, both a Gaussian ensemble distribution and a single-exponential correlation function.

The results we have found are in good agreement with the existing theoretical treatments.^{10,20,21} The techniques we have used, however, may open the way to similar joint measurements on more complicated scattering media, such as those in which the presence of long-range correlations or nonlinear phenomena destroys the Gaussian character of the ensemble distribution, or those in which the presence of more than one relaxation time gives a non-Lorentzian frequency profile.

ACKNOWLEDGMENTS

We cordially thank A. Sona and G. Potenza for useful comments, and the Dow Chemical Company for providing us with the scattering samples.